

Photoproduction of the 3π mesons in the reaction $\gamma p \rightarrow \pi^+\pi^+\pi^-n$ with CLAS detector at 6 GeV/ c^2

A. Tsaris,¹ P. Eugenio,¹ A. I. Ostrovidov,¹ and [other CLAS collaborators]²

¹⁾ *Physics Department, Florida State University*

²⁾ *Jefferson Lab*

(Dated: 15 July 2019)

We performed a study of the $\pi^+\pi^+\pi^-$ system photoproduced in the charge-exchange reaction $\gamma p \rightarrow \pi^+\pi^+\pi^-n$, with a special emphasis on the search for the exotic mesons. Data were collected during g12 run period of the CLAS spectrometer at Jefferson Lab. A 6 GeV/ c^2 tagged photon beam on a liquid hydrogen target was utilized. In order to enhance the peripheral production, events were selected with a low four-momentum transfer to the recoil neutron. A mass-independent partial wave analysis was performed on a sample of 600K events, the largest 3π photoproduction dataset published to date. In addition to the previously observed $a_2(1320)$ and $\pi_2(1670)$ states, the presence of the $a_1(1260)$ meson in the photoproduction is established for the first time. However, there is no evidence for the photoproduction of the exotic $J^{PC} = 1^{-+}$ meson with the $\rho\pi$ decay mode, which was claimed to be observed in the experiments with the incoming pion beams. The exotic $J^{PC} = 1^{-+}$ partial waves do not show any peaking intensity, and their phase motions relative to the resonant $\pi_2(1670)$ waves are consistent with a non-resonant behavior.

The standard quark model predicts the spectrum of the ordinary $q\bar{q}$ mesons. They are classified in terms of the J^{PC} multiplets, where J is the total angular momentum, P is the parity and C is the particle-antiparticle conjugation parity. These quantum numbers should satisfy the following relation:

$$\vec{J} = \vec{L} + \vec{S}, \quad P = (-1)^{L+1}, \quad C = (-1)^{L+S}, \quad (1)$$

where L is the relative orbital angular momentum between the quark and the antiquark, and S is the intrinsic parity of the $q\bar{q}$ pair. As a result, certain J^{PC} combinations are forbidden for a simple $q\bar{q}$ system. Quantum chromodynamics (QCD), however, allows for additional states in the presence of gluonic excitations. Due to the self-interacting nature of the gluon, such excitation can be considered as a constituent gluon on par with the constituent quarks. With an additional gluonic degree of freedom, all possible J^{PC} multiplet values are allowed for a hybrid $q\bar{q}g$ configuration, including "exotic" ones which are forbidden for ordinary mesons. Observing a state with such quantum numbers will serve as a direct signature of an exotic hybrid meson. In this report, we present the results of our search for a photoproduced exotic meson with a decay mode into three charged pions.

Recent lattice QCD calculations¹ predict that the lowest lying hybrid state will have $J^{PC} = 1^{-+}$ with a mass of about 1.9 GeV/ c^2 . In the framework of the QCD-inspired flux-tube model², the decay of hybrids into two S-wave mesons, such as the $\rho(770)\pi$ decay, will be suppressed in favor of a decay into an S-wave meson and a P-wave one, such as the $b_1(1235)\pi$ and the $f_1(1285)\pi$ decays. Nevertheless, the two S-wave decay mode for hybrids might not be negligible after all³.

Possible candidates for a light $J^{PC} = 1^{-+}$ exotic hybrid mesons have been seen by the E852, VES and COM-PASS collaborations in the peripheral π^-p interactions at different energies. Of special interest to our 3π analysis

is the $\pi_1(1600)$ state due to previous claims of its observation in the $\rho\pi^{4-7}$ decay mode, as well as in the $\eta'\pi^{8,9}$, $f_1(1285)\pi^{10,11}$ and $b_1(1235)\pi^{11,12}$ channels. It was also seen in the $p\bar{p} \rightarrow b_1(1235)\pi\pi$ analysis¹³. This state, however, is not yet solidly established. There may be other non-resonant interpretations of the observed 1^{-+} signal. Moreover, a different analysis of a larger $\rho\pi$ dataset from E852¹⁴ found no evidence for an exotic resonance at 1.6 GeV/ c^2 in the 3π final state.

There are theoretical reasons to assume¹⁵ that an incoming photon beam is more favorable for the production of the exotic hybrids than the pion one. There is even a prediction¹⁶ that the $\pi_1(1600)$ is expected to be photoproduced with a cross section similar to the $a_2(1320)$ meson. However, experimental photoproduction data are very scarce and rarely have sufficient statistics to perform an amplitude analysis. The CLAS-g6c run group at Jefferson Lab collected 83K $\gamma p \rightarrow n\pi^+\pi^+\pi^-$ events in 2001 and performed a partial-wave analysis¹⁷. No clear resonant structure has been observed in the intensities of the $J^{PC} = 1^{-+}$ exotic partial waves. However, photoproduction of the $\pi_1(1600)$ state at the same relative cross sections as reported in pion production could not be ruled out due to limited statistics and lack of the partial waves phase information.

To explore the photoproduction of the exotic hybrid mesons, the HyCLAS¹⁸ experiment was proposed in 2003. It took data during g12 run of the CLAS experiment at Jefferson Lab in 2008. A beam of circularly polarized tagged photons with the energy range from 1.2 to 5.4 GeV/ c^2 was produced via bremsstrahlung of a 5.7 GeV/ c^2 electron beam passing through a radiator. The CEBAF Large Acceptance Spectrometer (CLAS) is divided into 6 sectors azimuthally around the beam line and utilizes a large superconducting toroidal magnet for momentum measurement of the charged tracks. Each sector, covering $\frac{3}{4}\pi$ radians in azimuth, consists of a segmented scintillator start counter for timing and

triggering, three layers of the drift chambers for charged track reconstruction, a scintillator time-of-flight system and a gas Cherenkov counter for particle identification, and an electromagnetic calorimeter. Complete details of the CLAS spectrometer design can be found in Ref.¹⁹. The target, a cylindrical liquid hydrogen cell, was moved 90 cm upstream from its typical position at the center of CLAS in order to improve the acceptance for the forward-going fast pions and, therefore, optimize the detector for the higher-energy meson spectroscopy run.

From the 26 billion triggers collected by CLAS-g12, 700M events have three reconstructed charged pions. Timing and vertex cuts were applied to clean up the sample. Next, a missing neutron was identified via kinematic fitting. To suppress the s -channel processes, only events with the incoming beam energy above $4.4 \text{ GeV}/c^2$ were chosen, leaving 7.4M events after these steps. To enhance the peripheral production off a recoil neutron and suppress the production of the excited baryons, a selection on the small values of $|t'| = |t - t_0|$ was necessary. Here t is the four-momentum transfer squared from the incoming beam to the recoil, and t_0 is its minimum value allowed by kinematics for a given value of the 3π mass. The observed distribution of $|t'|$ follows the $e^{-b|t|}$ dependence expected for a single-pion t -channel exchange production. However, to eliminate the visible peaks from the excited baryon background in the πp and $\pi\pi p$ mass spectra, an additional θ_{lab} on the pion's lab angle was necessary. Specifically,

$$|t'| = |t - t_0| < 0.1 \text{ GeV}^2/c^4, \quad \theta_{lab}[\pi_{slow}^+] < 25^\circ \quad (2)$$

where π_{slow}^+ is the positive pion with the smaller magnitude of momentum.

After these cuts, the final $\gamma p \rightarrow n\pi^+\pi^+\pi^-$ data sample consisted of 600K events which were used in the partial wave analysis. We note that the measured slope b for the exponential t' distribution is equal to $14.39 \text{ (GeV}/c)^{-2}$ for the final sample. Figure 1 illustrates the main features of these events. The invariant mass of the 3π system (Fig. 1a) exhibits a clear peak at the mass of the $a_2(1320)$ meson, along with a broad enhancement in the $1.5\text{-}1.7 \text{ GeV}/c^2$ mass region. Fig. 1b shows the $\pi^+\pi^-$ invariant mass distributions, where the fast and slow pions are separated by the relative value of their momenta. The $\rho(770)$ intermediate isobar is seen for both $\pi^-\pi_{slow}^+$ and $\pi^-\pi_{fast}^+$ combinations, with an additional peak from the $f_2(1270)$ isobar for the fast pion. Dalitz plots for two different 3π -mass regions (below and above $1.5 \text{ GeV}/c^2$) are shown in Fig. 1c (low mass) and Fig. 1d (high mass). Again the ρ and f_2 intermediate $\pi\pi$ isobars are visible.

The data were binned in 20 MeV bins of the 3π mass to perform a mass independent partial wave analysis which, at its core, is the event based maximum likelihood fit. The decay amplitudes of partial waves were calculated using the helicity formalism in the reflectivity basis in the framework of the isobar model²⁰. They are

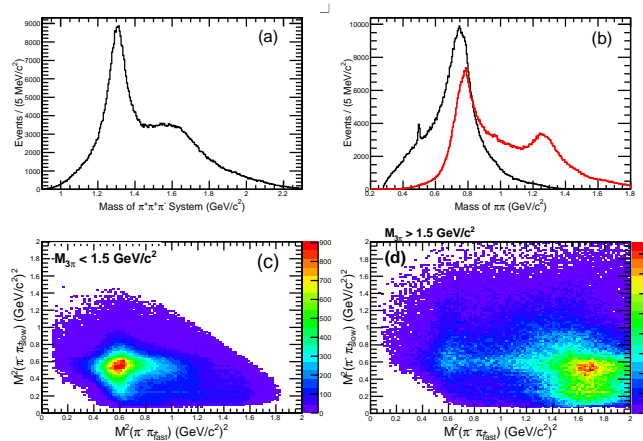


FIG. 1. Final event sample: (a) the 3π invariant mass; (b) the $\pi^-\pi_{fast}^+$ (red curve) and $\pi^-\pi_{slow}^+$ (black curve) invariant mass distributions; (c) Dalitz plot for $M_{3\pi} < 1.5 \text{ GeV}$ (low mass region); (d) Dalitz plot for $M_{3\pi} > 1.5 \text{ GeV}$ (high mass region).

symmetrized over two positive pions. Effects of the finite experimental acceptance were taken into account by means of the normalization integrals. To calculate them, t -channel Monte Carlo phase space events were generated and passed through the simulation of the CLAS detector. The mass-independent fit determined the unknown production amplitudes for each partial wave in each mass bin. They were used to calculate such observables as intensities and phases of the waves. As the final step, a mass-dependent Breit-Wigner fit of intensities and phases was performed to study a possible resonant nature of the waves.

The notation used to describe the partial waves is $J^{PC}M^\epsilon[Y\pi]_L$, where J is the total angular momentum, P is the parity, C is the C-parity, M is the projection of J , ϵ is the reflectivity, Y is the intermediate isobar with parameters from the PDG²¹, and L is the relative orbital angular momentum between the isobar and the bachelor pion. To achieve the acceptable quality of the fit, 13 partial waves were required in the 3π mass region below $1.38 \text{ GeV}/c^2$, and 17 partial waves in the high 3π mass region above that. The extra waves were due to the opening of the $f_2\pi$ mass threshold.

The list of partial waves in the final PWA fit is shown in Table I. Many other waves had been tried but were found to be insignificant. Also included was an isotropic non-interfering background wave to accommodate for the possible presence of misidentified events from other topologies in the final event sample. It was found that the production of all zero-projection $M = 0$ waves is strongly suppressed. This is consistent with a single-pion exchange mechanism because the helicity of a beam photon is never zero and the exchange particle is spinless. In addition, the pairs of waves with the same quantum numbers apart from the opposite reflectivities (i.e., $M^\epsilon = 1^+$ and $M^\epsilon = 1^-$ pairs) had roughly equal yields. This is

TABLE I. Partial waves used in the final PWA fit.

Partial waves for $M_{3\pi} < 1.38 \text{ GeV}$	
$J^{PC} = 1^{++}$:	$1^{\pm}[\rho\pi]_S, 1^{\pm}[\sigma\pi]_P, 1^{\pm}[\rho\pi]_D$
$J^{PC} = 1^{-+}$:	$1^{\pm}[\rho\pi]_P$
$J^{PC} = 2^{++}$:	$1^{\pm}[\rho\pi]_D$
$J^{PC} = 2^{-+}$:	$1^{\pm}[\rho\pi]_P$
Background	
Additional partial waves for $M_{3\pi} > 1.38 \text{ GeV}$	
$J^{PC} = 2^{-+}$:	$1^{\pm}[f_2\pi]_S, 1^{\pm}[f_2\pi]_D$

consistent with the fact that an unpolarized or circularly polarized beam has equal amounts of opposite linear polarizations. As a result, waves of opposite reflectivities should be produced equally regardless of the naturalness of the dominant exchange particle²². The goodness of fit was verified by comparing the experimentally observed angular and mass distributions with the predicted ones. The later were obtained by weighting phase space Monte Carlo events with a spin-density matrix found in a PWA fit, and by applying the effects of the simulated detector acceptance. All observed and predicted distributions were shown to be in very good agreement with each other²³.

The features of the most important partial waves are presented below. Figures 2a and 2b show the intensities of the $2^{++}1^{\pm}[\rho(770)\pi]_D$ and $1^{++}1^{\pm}[\rho(770)\pi]_S$ partial waves. The intensities are summed up over both reflectivities. The $J^{PC} = 2^{++}$ wave is the dominant one in the data. The mass dependent Breit-Wigner (BW) fit of the $J^{PC} = 2^{++}$ wave yields a mass of $M = 1.331 \pm 0.001 \text{ GeV}/c^2$ and a width of $\Gamma = 0.108 \pm 0.002 \text{ GeV}/c^2$ for the peak in the $2^{++}D$ wave. These values are consistent with the $a_2(1320)$ meson. The mass dependent BW fit of the $1^{++}S$ partial wave intensity yields a mass of $M = 1.169 \pm 0.004 \text{ GeV}/c^2$ and a width of $\Gamma = 0.29 \pm 0.02 \text{ GeV}/c^2$. The structure in this wave can be identified as the $a_1(1260)$ meson. Figures 2c and 2d show the phase difference between the $1^{++}S$ and $2^{++}D$ waves for $M^{\epsilon} = 1^{+}$ and $M^{\epsilon} = 1^{-}$. The curve shows the expected Breit Wigner phase difference between the $a_1(1260)$ and $a_2(1320)$ resonances with their parameters obtained in the mass dependent fit. The curves are in good agreement with the data in the resonant region. It is worth mentioning here that the $a_1(1260)$ meson has not been reported previously in charge-exchange photoproduction.

In the high 3π mass region above the $f_2(1270)\pi$ mass threshold, the dominant wave is the $2^{-+}1^{\pm}[f_2(1270)\pi]_S$ one. The combined intensity of the $2^{-+}1^{\pm}S$ waves is presented in Figure 3a. The mass dependent BW fit of this wave results in a mass of $M = 1.634 \pm 0.002 \text{ GeV}/c^2$ and a width of $\Gamma = 0.252 \pm 0.005 \text{ GeV}/c^2$, which is consistent with the well known $\pi_2(1670)$ meson. Figure 3b shows the combined intensity of the $1^{-+}1^{\pm}P$ exotic waves while its relative phase differences with the much stronger $2^{-+}S$ waves are shown in Figures 3c,d for

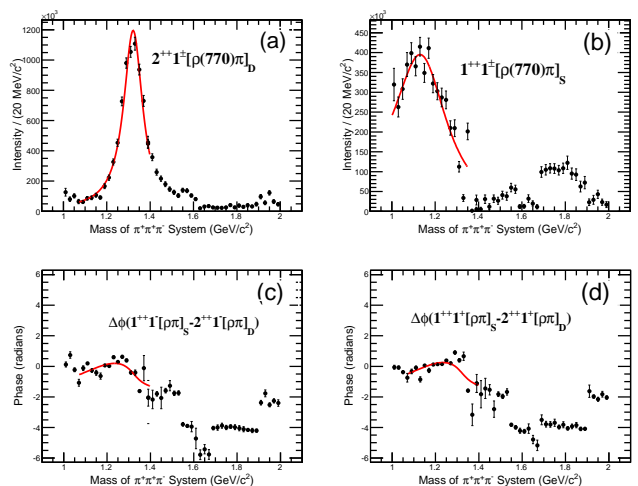


FIG. 2. (a,b): The intensities of the $2^{++}1^{\pm}[\rho(770)\pi]_D$ wave (a) and the $1^{++}1^{\pm}[\rho(770)\pi]_S$ wave (b) combined over $M^{\epsilon} = 1^{\pm}$ reflectivities. The curves show the mass dependent BW fit. (c,d): The relative phase differences between the $1^{++}S$ and $2^{++}D$ waves for $M^{\epsilon} = 1^{-}$ (c) and $M^{\epsilon} = 1^{+}$ (d) reflectivities. The curves show the expected BW phase difference with parameters from the mass dependent fit of intensities.

both $M^{\epsilon} = 1^{\pm}$ reflectivities. The curves on these plots demonstrate the expected BW behavior for 3 different assumptions about the resonant nature of the exotic 1^{-+} wave while the $2^{-+} \pi_2(1670)$ reference wave is always assumed to be resonating with parameters obtained in the BW fit of its intensity. The red curve corresponds to the assumption of a non-resonating exotic wave. In the case of the dashed blue line, the 1^{-+} is assumed to be resonant with parameters reported by the E852 group in the 3π decay mode⁵ of the $\pi_1(1600)$ exotic candidate. For a solid blue line, the $\pi_1(1600)$ parameters are taken from the E852 report on the $\eta'\pi$ decay mode⁹ where the observed $\pi_1(1600)$ state was dominant but somewhat broader. One may conclude that the measured phase difference along with the absence of a clear structure in the intensity strongly favors a non-resonant $1^{-+}P$ behavior.

As an additional check, the $1^{-+}P$ exotic waves were compared with the $2^{-+}1^{\pm}D$ waves whose combined intensity can be seen in Figure 4a. This is the D -wave mode of the $\pi_2(1670)$ decay. The $1^{-+}P$ wave phase motions for 2 reflectivities are in Figures 4b,c. Once again, the phase motion is non-resonant in respect to the D -wave amplitudes of the $\pi_2(1670)$ resonance in the same way as versus the S -wave amplitudes.

To summarize, we performed a partial wave analysis of the reaction $\gamma p \rightarrow \pi^+\pi^+\pi^-n$ at $5.4 \text{ GeV}/c^2$. We observed the well known $a_2(1320)$, $\pi_2(1670)$ and, for the first time in photoproduction, $a_1(1260)$ resonances. However, neither the intensity nor the phase motion of the $J^{PC} = 1^{-+}$ exotic partial wave indicates the charge-exchange photoproduction of the $\pi_1(1600)$ hybrid meson candidate.

The authors gratefully acknowledge the excellent sup-

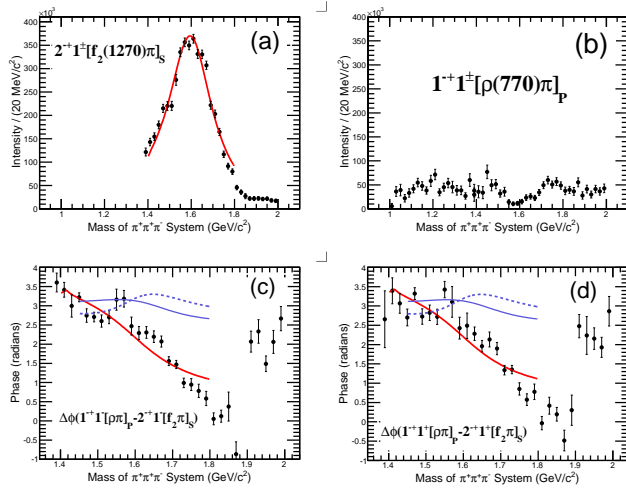


FIG. 3. (a,b): Combined intensities of the $2^{-+}1^{\pm}[f_2(1270)\pi]_S$ (a) and $1^{-+}1^{\pm}[\rho(770)\pi]_P$ (b) waves. The mass dependent of the 2^{-+} wave intensity is shown with the curve; (c,d): The relative phase differences of the exotic $1^{-+}P$ waves against the $2^{-+}S$ waves for $2 M^{\epsilon} = 1^{\pm}$ reflectivities. The curves represent the expected phase difference against a resonating $\pi_2(1670)$ state for the 3 assumptions of a non-resonating exotic wave (red curve), a resonating $\pi_1(1600)$ state with the E852 parameters for the 3π decay (dashed blue curve), and a resonating $\pi_1(1600)$ state with the E852 parameters for the $\eta'\pi$ decay (solid blue curve).

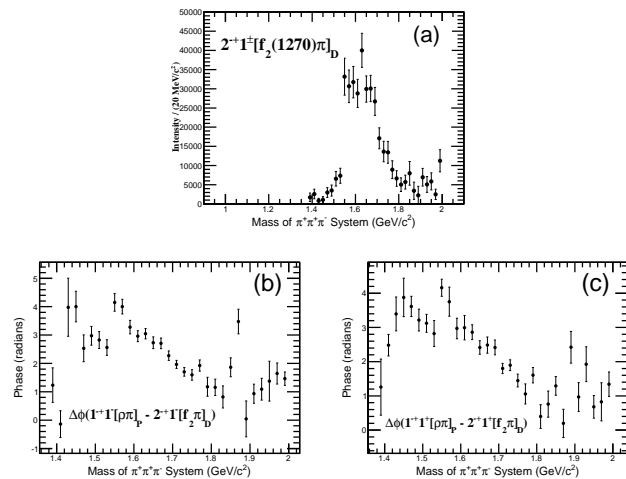


FIG. 4. (a) The combined intensity of the $2^{-+}1^{\pm}[f_2(1270)\pi]_D$ partial wave. (b,c): The phase differences of the exotic $1^{-+}P$ wave against the $2^{-+}D$ wave for the positive (b) and negative (c) reflectivities.

port of the technical staff at Jefferson Lab and all participating institutions. This research is based on work supported by the U.S. Department of Energy, Office of Science, Office of Nuclear Physics, under Contract No. DE-AC05-06OR23177. The group at Florida State University acknowledges additional support from the U.S. Department of Energy, Office of Science, Office of Nuclear Physics, under Contract No. DE-FG02-92ER40735. This work was also supported by the U. S. National Science Foundation, the State Committee of Science of Republic of Armenia, the Chilean Comisión Nacional de Investigación Científica y Tecnológica, the Italian Istituto Nazionale di Fisica Nucleare, the French Centre National de la Recherche Scientifique, the French Commissariat à l'Énergie Atomique, the Scottish Universities Physics Alliance (SUPA), the United Kingdom Science and Technology Facilities Council (STFC), the National Research Foundation of Korea, the Deutsche Forschungsgemeinschaft (SFB/TR110), the Russian Science Foundation under Grant No. 16-12-10267, and the National Natural Science Foundation of China under Grants No. 11475181 and No. 11635009.

¹Jozef J. Dudek, Phys. Rev. D **84**, 074023 (2011).

²Nathan Isgur and Jack E. Paton, Phys. Rev. D **31**, 2910 (1985).

³E. S. Swanson P. R. Page and A. P. Szczepaniak, Phys. Rev. D **59**, 034016 (1999).

⁴G. S. Adams *et al.*, Phys. Rev. Lett. **81**, 5760 (1998).

⁵S. U. Chung *et al.*, Phys. Rev. D **65**, 072001 (2002).

⁶Y. Khokhlov, Nucl. Phys. A **663-664**, 596c (2000).

⁷M. Alekseev *et al.*, Phys. Rev. Lett. **104**, 2010 (241803).

⁸G. M. Beladidze *et al.*, Phys. Lett. B **313**, 276 (1993).

⁹E. I. Ivanov *et al.*, Phys. Rev. Lett. **86**, 3977 (2001).

¹⁰J. Kuhn *et al.*, Phys. Lett. B **595**, 109 (2004).

¹¹D. V. Amelin *et al.*, Phys. At. Nucl. **68**, 359 (2005).

¹²M. Lu *et al.*, Phys. Rev. Lett. **94**, 032002 (2005).

¹³C. A. Baker *et al.*, Phys. Lett. B **563**, 140 (2003).

¹⁴A. Dzierba *et al.*, Phys. Rev. D **73**, 072001 (2006).

¹⁵F. Close and P. Page, Phys. Rev. D **52**, 1706 (1995).

¹⁶A. Szczepaniak and M. Swat, Phys. Lett. B **516**, 72 (2001).

¹⁷M. Nozar *et al.*, Phys. Rev. Lett. **102**, 102002 (2009).

¹⁸Paul Eugenio *et al.*, CLAS Analysis Proposal PR04-005 (Jefferson Lab, 2003).

¹⁹B. A. Mecking *et al.*, Nucl. Instrum. Methods Phys. Res. A **503**, 513 (2003).

²⁰S. U. Chung, Formulas for Partial-Wave Analysis BNL-QGS-06-102 (Brookhaven Lab, 2014).

²¹C. Patrignani *et al.* (Particle Data Group), Chin. Phys. C **40**, 100001 (2016).

²²Paul Eugenio, Int. Jour. of Mod. Phys. A **18**, No 3, 487 (2003).

²³Aristeidis Tsaris, PhD dissertation, Florida State University (2016).